

# Magnetic reconnection at 3D null points: effect of magnetic field asymmetry

A. K. Al-Hachami and D. I. Pontin

Division of Mathematics, University of Dundee, U.K.

## Abstract

The magnetic field in many astrophysical plasmas, for example in the solar corona, is known to have a highly complex – and clearly three-dimensional – structure. Turbulent plasma motions in high- $\beta$  regions where field lines are anchored, such as the solar interior, can store large amounts of energy in the magnetic field. This energy can only be released when magnetic reconnection occurs. Reconnection may only occur in locations where huge gradients of the magnetic field develop, and one candidate for such locations are magnetic null points, known to be abundant for example in the solar atmosphere. Reconnection leads to changes in the topology of the magnetic field, and energy released as heat, kinetic energy and acceleration of particles. Thus reconnection is responsible for many dynamic processes, for instance flares and jets. The aim of this paper is to investigate the properties of magnetic reconnection at a 3D null point, with respect to their dependence on the symmetry of the magnetic field around the null. In particular we examine the rate of flux transport across the null point with symmetric/asymmetric diffusion regions, as well as how the current sheet forms in time, and its properties. Mathematical modelling and finite difference resistive MHD simulations. It is found that the basic structure of the mode of magnetic reconnection considered is unaffected by varying the magnetic field symmetry, that is, the plasma flow is found cross both the spine and fan of the null. However, the peak intensity and dimensions of the current sheet are dependent on the symmetry/ asymmetry of the field lines. As a result, the reconnection rate is also found to be strongly dependent on the field asymmetry. The symmetry/asymmetry of the magnetic field in the vicinity of a magnetic null can have a profound effect on the geometry of any associated reconnection region, and the rate at which the reconnection process proceeds.

## 1 Introduction

Magnetic reconnection is the breaking and topological or geometrical rearrangement of the magnetic field lines in a plasma. The magnetic field plays

a fundamental role in many of the phenomena that occur in the plasma. It is not surprising that three-dimensional (3D) magnetic fields are more complex than the two-dimensional. It is known from observations that magnetic reconnection occurs in abundance in astrophysical plasmas. However, due to the very low plasma resistivity, reconnection may only occur where very intense currents ('current sheets') develop. One of the most fundamental questions that must be answered to determine the locations and mechanisms of energy release in astrophysical plasmas is therefore: where may such currents develop?

It is now becoming clear that the magnetic field in the solar atmosphere has a highly complex structure. Two major candidates that have been proposed as sites of current sheet formation in such a complex magnetic field are 3D nulls points, and associated separator field lines (Lau and Finn, 1990; Klapper et al., 1996; Priest and Titov, 1996; Longcope and Cowley, 1996; Galsgaard and Nordlund, 1997; Pontin and Craig, 2005; Longcope, 1996, 2001) field lines that link two nulls. We focus here on reconnection at isolated 3D nulls. Indications are that an abundance of 3D nulls is present in the solar corona (Schrijver and Title, 2002; Longcope et al., 2003), which have been suggested as likely sites for coronal heating (e.g. Priest et al., 2005). Moreover, recent observations suggest that reconnection at such nulls may play an important role in solar flares (e.g. Fletcher et al., 2001; Luoni et al., 2007) and coronal mass ejections (e.g. Ugarte-Urra et al., 2007; Barnes, 2007). Furthermore, recently the first in-situ observations have been made by the Cluster spacecraft of single and multiple 3D magnetic nulls in the Earth's magnetotail (e.g. Xiao et al., 2006). The observations further suggest that these nulls may be playing an important role in the reconnection process occurring in the magnetotail. Though magnetic field measurements in other astrophysical objects further afield are difficult, it is almost certain that similar reconnection processes at 3D nulls also occur there.

To find the local magnetic structure about a null point, we consider the magnetic field in the vicinity of null point where the field vanishes ( $\mathbf{B}=0$ ). If the null point is taken to be situated at the origin and, in addition, assume you are sufficiently close to null point may be expressed as

$$\mathbf{B} = \mathcal{M} \cdot \mathbf{r} \tag{1}$$

where  $\mathcal{M}$  is a matrix with the elements of the Jacobian of  $\mathbf{B}$  and  $\mathbf{r}$  is the position vector  $(x, y, z)^T$ . The eigenvalues of  $\mathcal{M}$  sum to zero since  $\nabla \cdot \mathbf{B} = 0$ . We consider the situation where all the eigenvalues are real. Since they sum to zero there is always one eigenvalue of opposite sign to the other two. The two eigenvectors corresponding to the eigenvalues with same-sign real

part define the “fan surface” of the null. The third eigenvector defines the orientation of the “spine line”. For more details, see e.g. Fukao et al. (1975); Lau and Finn (1990); Parnell et al. (1996).

Unlike in two dimensions, reconnection can occur in 3D either at a null point or in the absence of nulls (Schindler et al., 1988; Priest and Forbes, 2000; Demoulin, 2006). What’s more, the nature of reconnection in 3D has been shown to be fundamentally different from 2D reconnection (Priest et al., 2003). The nature of magnetic reconnection in the absence of a three-dimensional null point has been discussed by Hesse (1991) and Hornig and Priest (2003). The kinematics of steady reconnection at three dimensional null points have been studied by Priest and Titov (1996) when  $\eta = 0$ . Later, Pontin et al. (2004, 2005) improved this model by adding a finite resistivity, localised around the null point. Two distinct cases were considered, in which the current ( $\mathbf{J}$ ) was directed parallel to first the spine and second the fan plane of the null. The structures of the two solutions were found to differ greatly, and as a result, the reconnection rate, calculated by integrating the  $E_{\parallel}$  along field lines, represents very different behaviors of the flux for the two cases. In the first case, in which  $\mathbf{J}$  was directed parallel to the spine, a type of rotational flux mis-matching was found, with no flow being present across either the spine or the fan of the null point. On the other hand, when  $\mathbf{J}$  was directed parallel to the fan surface, it was found that magnetic flux is transported through the spine line and the fan plane, in a process much more conceptually similar to the 2D case. In this case it can be shown that the reconnection rate gives a measure of the rate of flux transport across the separatrix surfaces(s) of the null (Pontin et al., 2005). In each of these investigations only the azimuthally symmetric case was considered, that is the case in which the magnetic field in the fan plane is isotropic. In this paper we focus on the case where  $\mathbf{J}$  is parallel to the fan surface, and for the first time consider magnetic reconnection at a generic non-symmetric magnetic null point. The different modes of reconnection that occur in practice in a plasma (when the full set of MHD equations are considered) have recently been classified by Priest and Pontin (2009). In terms of the framework they have set up, the mode of reconnection considered here is termed *spine-fan reconnection*.

In section 2, we describe a kinematic model for reconnection at a non-symmetric null point, comparing our results with those of Pontin et al. (2005). In section 4 we describe the results of a related resistive magnetohydrodynamic (MHD) numerical simulation, and in section 5 we present our conclusions.

## 2 Kinematic solution

### 2.1 The model

The subject of magnetic reconnection is a complex subject, and its study is still in the early stages. Therefore, one approach that is used to try to understand the properties of this process is to consider a reduced set of the MHD equations. There are a number of analytical 3D solutions, which are described by Hornig and Priest (2003) and Wilmot-Smith et al. (2006, 2009), where there is no null point of the magnetic field, as well as the solutions in the presence of a null mentioned above (Pontin et al., 2004, 2005). These solutions are kinematic reconnection, that is they satisfy Maxwell's equations, as well as the induction equation. We seek a solution to the kinematic, steady, resistive MHD equations in the locality of a magnetic null point. That is, we solve

$$\mathbf{E} + \mathbf{v} \times \mathbf{B} = \eta \mathbf{J} \quad (2)$$

$$\nabla \times \mathbf{E} = \mathbf{0} \quad (3)$$

$$\nabla \times \mathbf{B} = \mu_0 \mathbf{J} \quad (4)$$

$$\nabla \cdot \mathbf{B} = 0 \quad (5)$$

As discussed above, here we consider a null point with current directed parallel to the fan plane. We choose the magnetic field to be

$$\mathbf{B} = \frac{B_0}{L} \frac{2}{p+1} (x, py - jz, -(p+1)z) \quad (6)$$

where  $p$  is a parameter. This generalises the previous work by Pontin et al. (2005), who considered only the azimuthally symmetric case, corresponding to  $p = 1$ . For convenience we will write  $2B_0/L(p+1) = B'_0$ . The current lies in the  $x$ -direction, and is given by  $\mathbf{J} = (B'_0/\mu_0)(j, 0, 0)$  from (4). Examining the matrix  $\mathcal{M}$  (see Eq. 1), the eigenvalues of the null point are found to be

$$\lambda_1 = B'_0, \quad \lambda_2 = pB'_0, \quad \lambda_3 = -(p+1)B'_0$$

with corresponding eigenvectors

$$\mathbf{k}_1 = (1, 0, 0), \quad \mathbf{k}_2 = (0, 1, 0), \quad \mathbf{k}_3 = \left(0, 1, \frac{2p+1}{j}\right)$$

It is clear from the above that the fan plane defined by  $\mathbf{k}_1$  and  $\mathbf{k}_2$ . The fan plane of this magnetic null point is coincident with the plane  $z = 0$  (here we

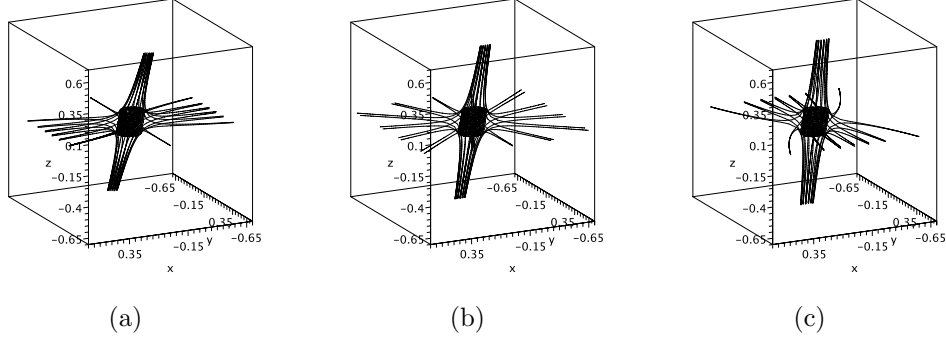


Figure 1: The structure of null point with different values of  $p$ : (a)  $p = 0.5$ , (b)  $p = 1$  and (c)  $p = 2$ .

restrict ourselves to the case  $p > 0$ ) while the spine is not perpendicular to this, but rather lies along  $x = 0, y = jz/(2p + 1)$  (see figure 1).

For the chosen magnetic field (6), closed-form expressions for the equations of magnetic field lines can be found, by solving

$$\frac{\partial \mathbf{X}(s)}{\partial s} = \mathbf{B}(\mathbf{X}(s)), \quad (7)$$

where the parameter  $s$  runs along field lines, to give

$$x = x_0 e^{B'_0 s} \quad (8)$$

$$y = \left( y_0 - \frac{jz_0}{2p+1} \right) e^{pB'_0 s} + \frac{jz_0 e^{-B'_0(p+1)s}}{2p+1} \quad (9)$$

$$z = z_0 e^{-B'_0(p+1)s} \quad (10)$$

The inverse of equations (8,9,10) are

$$x_0 = x e^{-B'_0 s} \quad (11)$$

$$y_0 = \frac{(2pye^{(-B'_0 ps)} + ye^{(-B'_0 ps)} + jze^{(B'_0(p+1)s)} - jze^{(-B'_0 ps)})}{2p+1} \quad (12)$$

$$z_0 = ze^{B'_0(p+1)s} \quad (13)$$

which describes the equations of the magnetic field lines in terms of some initial coordinates  $\mathbf{X}_0 = (x_0, y_0, z_0)$ .

We proceed to solve (2-5) as follows. From equation (3) we can write, in general  $\mathbf{E} = -\nabla\phi$  where  $\phi$  is a scalar potential. Then the component

of equation (2) parallel to  $\mathbf{B}$  is  $-(\nabla\phi)_{\parallel} = \eta\mathbf{J}_{\parallel}$  and we can calculate  $\phi$  by integrating along magnetic field lines:

$$\phi = - \int \eta \mathbf{J} \cdot \mathbf{B} ds + \phi_0 \quad (14)$$

where  $\phi_0$  is a constant of integration. By substituting the equations (8,9,10) into the integrand of Eq. (14), we can perform this integration to obtain  $\phi(\mathbf{X}_0, s)$ . Once this is done, we use equations (11,12,13) to eliminate  $s, x_0$  and  $y_0$  to obtain  $\phi(\mathbf{X})$ , treating  $z_0$  as a constant (see below). The electric field can subsequently be found from

$$\mathbf{E} = -\nabla\phi \quad (15)$$

and we then find the plasma velocity perpendicular to the magnetic field  $\mathbf{v}_{\perp}$ , by taking the vector product of equation (2) with  $\mathbf{B}$  to obtain

$$\mathbf{v}_{\perp} = \frac{(\mathbf{E} - \eta\mathbf{J}) \times \mathbf{B}}{B^2} \quad (16)$$

Now, in order to investigate the properties of magnetic reconnection in a fully 3D system, we impose a resistivity model which ensures that the diffusion region is spatially localised in 3D. This is also the case relevant to astrophysical plasmas, which are known to be effectively ideal except in very small regions where energy release occurs. The diffusion region is chosen to be localised around the null point, in line with the results of past work which has shown that shearing motions tend to focus current in the vicinity of the null (Rickard and Titov, 1996; Pontin and Galsgaard, 2007; Pontin et al., 2007). Since the current is uniform in our simple model, we choose the resistivity to be localised, and take it to be of the form

$$\eta = \eta_0 \begin{cases} \left(\frac{R^2}{a^2} - 1\right)^2 \left(\frac{(z^2)^{\frac{2p}{p+1}}}{b^2} - 1\right)^2 & R^2 < a^2, (z^2)^{\frac{2p}{p+1}} < b^2 \\ 0 & \text{otherwise} \end{cases} \quad (17)$$

where  $R = \sqrt{(x^2)^p + (y - jz/(2p+1))^2}$  and  $\eta_0, a$  and  $b$  are constants.  $\eta_0$  is the value of  $\eta$  at the null point, and the diffusion region is a tilted cylinder centered on the spine axis ( $z$ -axis), extending to  $z = \pm b^{(p+1)/2p}$ . The cross-section of the diffusion region in the  $z = 0$  plane is circular with radius  $a$  when  $p = 1$ , but when  $p \neq 1$ , it extends to  $x = \pm a^{1/p}$  and  $y = \pm a$ . We choose this form of resistivity because it facilitates our method of solution by ensuring that every field line enters the diffusion region from above/below (in  $z$ ) and exits through the curved surface of the (generalised) cylinder.

In order to integrate Eq. (14), we must choose a surface on which to start our integration ( $s = 0$ ) that intersects each field line once and only once. We choose surfaces above and below the fan surface,  $z = \pm z_0$ , constant. Performing the calculation of  $\phi(\mathbf{X})$  as described above yields two expressions for  $\phi$ , for  $z > 0$  and  $z < 0$ . In order to match these two expressions in the fan plane, that is for  $\phi$  to be smooth and continuous, and thus physically acceptable, we must set the value of  $\phi$  at  $z = \pm z_0$  (i.e.  $\phi_0$ ) to be

$$\phi_0 = \frac{(32b^8p^2 + 16pb^{\frac{2(5p+3)}{p+1}} + 4pb^{\frac{4(3p+1)}{p+1}} - 12b^8p + b^8 - 2b^{\frac{2(5p+3)}{p+1}} + b^{\frac{4(3p+1)}{p+1}})\eta_0\frac{2B_0}{p+1}jx_0(\frac{z_0}{b})^{1/p+1}}{b^8(-1 + 8p)(4p - 1)} \quad (18)$$

$\phi(\mathbf{X})$ ,  $\mathbf{E}$  and  $\mathbf{v}_\perp$  can be obtained from (14), (15) and (16), as described earlier. The mathematical expressions are too lengthy to show here but can be calculated in a straightforward way using a symbolic computation package.

### 3 Analysis

#### 3.1 Nature of reconnection

In order to determine the structure of the magnetic reconnection process, we will examine the plasma velocity perpendicular to the magnetic field ( $\mathbf{v}_\perp$ ). This velocity transports the magnetic flux outside the diffusion region. The flow in  $x$ -direction does not cross the spine and is negligible for the reconnection process. However, in the  $yz$ -plane, the plasma flow crosses both the spine and the fan. Note that this is very similar to the situation described by Pontin et al. (2005) in the case of  $p = 1$ , the nature of plasma flow in a plane of constant  $x$  with the different values of  $p$  is shown in Fig. 2. Note that the qualitative structure – of a stagnation-point flow – is not affected a great deal by varying  $p$ , except at extreme values. However the general trend is that as  $p$  tends to zero, the plasma flow across the fan plane becomes weaker, see Fig. 2(a). We will return to discuss this behaviour below.

#### 3.2 Rate of reconnection

It is generally accepted that magnetic reconnection plays a fundamental role in many types of explosive astrophysical phenomena, for example solar flares. Yet what determines the reconnection rate is still a major problem and this is an important aspect of any reconnection model. In general, the reconnection

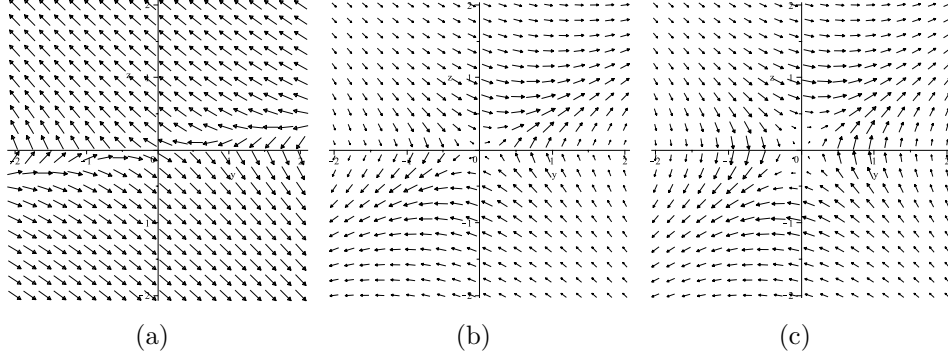


Figure 2: The structure of plasma flow across the spine and fan in typical plane of constant  $x$ , for (a)  $p = 0.2$ , (b)  $p = 0.9$ , (c)  $p = 2.5$ , for parameters  $\eta_0 = B_0 = j = a = b = L = 1$

rate in 3D is defined by the maximal value of

$$F = \int E_{\parallel} ds \quad (19)$$

along any field line threading the diffusion region  $D$  (e.g. Schindler et al., 1988). By symmetry, in this case

$$F = \int_{C2} E_{\parallel} ds \quad (20)$$

where the curve  $C2$ , as shown in figure 3, we define  $F$  as the reconnection rate. Since the fan is a flux surface, the integral may equally well be performed along the curve  $C1$ , the curve  $C1$  lying in the fan perpendicular to  $\mathbf{B}$ , see Fig. 3. Now, since the curve  $C1$  lies outside  $D$  and therefore, along it  $\mathbf{v} \times \mathbf{B} = -\mathbf{E}$ , we can write

$$F = \int_{C1} \mathbf{v} \times \mathbf{B} \cdot d\mathbf{l} \quad (21)$$

from which it is clear that this reconnection rate measures the rate at which flux is transported across the fan surface by the flow in the ideal region (Pontin et al., 2005).

From equation (20), we have

$$\begin{aligned} F &= - \int_{C2} E_x dx \\ &= \frac{2j \left( \frac{2B_0}{p+1} \right) \eta_0 (a + 6ap + 8ap^2 + a^{4p-3} + 2pa^{4p-3} - 2a^{2p-1} - 8pa^{2p-1})}{\mu_0(1+4p)(1+2p)} \end{aligned} \quad (22)$$



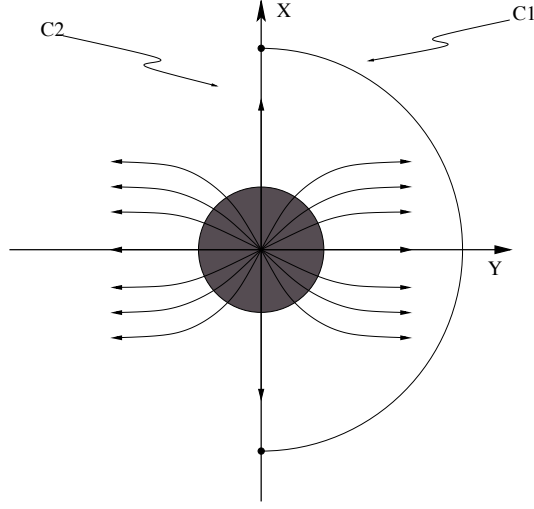


Figure 3: The curves C1 and C2 joining two points on the  $x$ -axis

Note as a point of verification that this reduces to the expression found by Pontin et al. (2005) when  $p = 1$ . Here we consider the dependence of the reconnection rate on the parameter  $p$  in two distinct cases—see Fig. 4. First we set the parameter  $j$  to be a constant,  $j = j_0$  say, which results in a current which is dependent on  $p$ . We then go on to consider the case where we set  $j = j_0(p + 1)$ , so that the current  $\mathbf{J}$  is independent of  $p$ .

We will also consider the effect, in each of these cases, of taking different values for the parameter  $a$ , which controls the dimensions of the diffusion region. When  $a = 1$ , the diffusion region is symmetric for all  $p$ , having circular cross-section in any plane of constant  $z$ . However, as stated above, the boundary of the diffusion region intersects each of the 3 coordinate axes at

$$x = \pm a^{1/p} \quad y = \pm a, \quad z = \pm b. \quad (23)$$

Thus the diffusion region becomes asymmetric when  $a \neq 1$  and  $p \neq 1$ . It will be seen later that this property is advantageous when comparing with the results of a numerical simulation.

### 3.2.1 Reconnection rate as $p \rightarrow \infty$

In the limit  $p \rightarrow \infty$ , we observe from (23) that the diffusion region becomes approximately symmetric (exactly symmetric if  $a = 1$ ). The following all holds for all values of  $a$ . For the two choices of dependence for our parameter

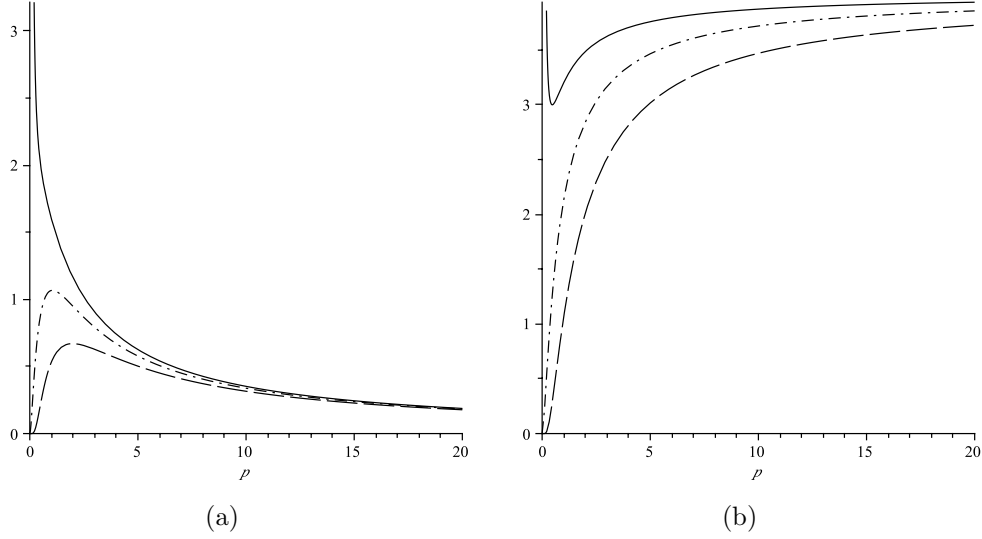


Figure 4: Dependence of the reconnection rate on  $p$ , where the solid curve at  $a > 1$ , dashed dot curve at  $a = 1$ , long dashed at  $a < 1$ , for parameters  $\eta_0 = 1$ ,  $B_0 = 2/(p + 1)$  and (a)  $j = j_0$ , (b)  $j = j_0(p + 1)$ .

$j$  stated above, evaluating Eq. (22) we find

$$\lim_{p \rightarrow \infty} F \Big]_{j=j_0} = 0 \quad (24)$$

$$\lim_{p \rightarrow \infty} F \Big]_{j=j_0(p+1)} = \frac{4j_0 B_0 \eta_0}{L \mu_0} \quad (25)$$

Consider first the case where the parameter  $j$  is chosen to be a constant,  $j = j_0$  (so that the  $\mathbf{J} = (B_0/L(p + 1)\mu_0) \hat{\mathbf{x}}$ ). The magnetic field in this case is  $\mathbf{B} \rightarrow (2B_0/L)(0, y, -z)$ . That is, the magnetic field approaches a 2D X-point structure with zero current, and so the result above ( $F \rightarrow 0$ ) is as expected. By contrast the reconnection rate approaches a constant value as  $p \rightarrow \infty$  when  $j = j_0(p + 1)$  (so that the  $\mathbf{J} = (B_0/L\mu_0) \hat{\mathbf{x}}$ ). In this case the magnetic field is  $\mathbf{B} \rightarrow (2B_0/L)(0, y - j_0 z, -z)$ . So the configuration is that of a 2D X-point with a uniform current (proportional to  $j_0$ ). As the diffusion region have only a finite extent along the direction of the current ( $\hat{\mathbf{x}}$ ), the reconnection rate is finite. Note that it is proportional to the parameters there are  $\eta_0, B_0, L, j_0$ , where  $\eta_0$  is the resistivity at the null, and  $2B_0 j_0/L\mu_0$  is the current modulus.

### 3.2.2 Reconnection rate as $p \rightarrow 0$

We now turn to the opposite limit;  $p \rightarrow 0$ . Note that our two parameter choices  $j = j_0$  and  $j = j_0(p+1)$  clearly reduce to one single value as the limit is approached. Setting  $p = 0$  the magnetic field is  $\mathbf{B} = (2B_0/L)(x, -j_0z, -z)$ . We note that this field contains a neutral line in 3D (along  $y = 0$ ) which is anti-parallel to the direction of current flow—not a configuration associated with 2D reconnection. In fact the limit of Eq. (22) is not well defined for all choices of our parameters. Therefore we consider that  $p = 0$  is not a physically relevant parameter choice and consider only the limit  $p \rightarrow 0$ .

As  $p \rightarrow 0$ , the magnetic field in the fan plane parallel to the current vector becomes strong, while the  $\hat{\mathbf{y}}$ -component becomes weak. Correspondingly, the flow across the fan surface becomes isolated to a small region near the fan, and weakens, see Fig. 2. Furthermore, in this case the diffusion region  $D$  is highly anti-symmetric. For  $a < 0$  the extent of  $D$  along the  $x$ -axis (direction of current flow) shrinks to zero. However, the reconnection rate also approaches zero when  $p \rightarrow 0$  even for the symmetric case ( $a = 1$ ). The reason for this can be understood by considering the fact that the profile of  $\eta$  is dependent on  $p$  in the model. When  $a = 1$ ,  $D$  also shrinks to zero in practical terms—although the boundary is still at  $x = \pm a$ , the resistivity becomes very small everywhere except right at the null (see Eq. 17). For  $a > 0$  this effect is still present, but is counteracted by the boundaries of  $D$  stretching to infinity (see Eq. (23)). Evaluating Eq. (22) we find

$$\lim_{p \rightarrow 0} F \Big]_{a \leq 1} = 0 \quad (26)$$

$$\lim_{p \rightarrow 0} F \Big]_{a > 1} = \infty \quad (27)$$

For  $a \leq 0$ , the diffusion region is either symmetric or shrinks to zero. The result of the weak flow across the fan for small  $p$  is that the reconnection rate also becomes very small. By contrast, for  $a > 1$ , the reconnection rate  $F \rightarrow \infty$ . Although the flow is still very weak across the fan, the diffusion region now has much larger extent in the  $x$ -direction, and so although the flux reconnected per unit length in that direction decreases, the total flux reconnected increases.

The results discussed above show that depending on our choice of parameters there are various different ways in which the reconnection rate may depend on the asymmetry of the field ( $p$ ). We now go on to perform simulations in the resistive MHD regime, in order to investigate which of these dependencies is relevant in a dynamically evolving plasma.

## 4 Resistive MHD simulations

### 4.1 Computational setup

We now proceed to test the results of the mathematical model presented in the previous section by performing numerical simulations which solve the full set of resistive MHD equations. We solve the MHD equations in the following form

$$\mathbf{E} = -\mathbf{v} \times \mathbf{B} + \eta \mathbf{J} \quad (28)$$

$$\mathbf{J} = \nabla \times \mathbf{B} \quad (29)$$

$$\frac{\partial \mathbf{B}}{\partial t} = -\nabla \times \mathbf{E} \quad (30)$$

$$\frac{\partial \rho}{\partial t} = -\nabla \cdot (\rho \mathbf{v}) \quad (31)$$

$$\frac{\partial}{\partial t}(\rho \mathbf{v}) = -\nabla \cdot (\rho \rho \mathbf{v} + \tau) - \nabla P + \mathbf{J} \times \mathbf{B} \quad (32)$$

$$\frac{\partial e}{\partial t} = -\nabla \cdot (e \mathbf{v}) - P \nabla \cdot \mathbf{v} + Q_{visc} + Q_J, \quad (33)$$

where  $\mathbf{v}, \mathbf{B}, \mathbf{E}, \eta, \mathbf{J}, \rho, \tau, P, e, Q_{visc}, Q_J$  are the velocity, magnetic field, electric field, resistivity, electric current, the density, the viscous stress, the pressure, the internal energy, the viscous dissipation and the Joule dissipation respectively. Now we need to explain the numerical simulations in the three dimension resistive MHD model. We use the simulations which were similar to that described by Pontin et al. (2007). We consider an isolated three dimension null point within our computational volume, which is driven from the boundary. We begin initially with a potential null point.

$$\mathbf{B} = \frac{B_0}{L} \frac{1}{p+1} (-(p+1)x, y, pz) \quad (34)$$

taking  $B_0=L=1$  and  $\eta=0.0007$ , constant, throughout. The computational domain has dimensions  $[x, y, z] = [-3 \dots 3, -3 \dots 3, -0.5 \dots 0.5]$ , with the magnetic field being line tied on all boundaries. In the kinematic model in the begin the spine and fan plane non orthogonal, but in the our simulation at the outset they are orthogonal, that is means the plasma is in equilibrium. At  $t = 0$ , the spine of the null point is lies on  $z$ -direction, and the fan plane with the  $z = 0$  plane. A driving velocity is then assumed on the  $z$ -boundaries, which advect the spine footpoints in opposite directions on the opposite boundaries. The spine is driven until the resulting disturbance reaches the null, resulting in formation a current sheet as the magnetic field becomes stressed and distorted. The driving velocity is then reduced back to

zero. For more details, see e.g. Pontin et al. (2007). In this work we compare between the kinematic solution and our simulation result.

## 4.2 Current sheet

In order to simplify the discussion we will initially explain the behavior of current at one value of  $p$  ( $p = 2$ ). It is importance to examine the temporal evolution of current in the volume. We can notice in the begin the spine and fan are orthogonal i.e. in the early evolution, but then this angle begin to change even reach to the maximum value to form the current sheet. In the other words the null collapses from an  $X$ - type null point to  $Y$ - type null point, see Fig. 5. After the driving velocity ceases the current begins to decrease again, and the spine and fan relax back towards their initial perpendicular state, see Fig. 7(a).

We go on to investigate the process of current sheet formation at such a 3D null point in the simulations with the different values of  $p$  and time dependence. We now discuss how the current sheet formation, as mentioned above, depends on the value of  $p$ . Fig. 6 illustrates the dimensions of the current sheet for various values of  $p$  at the time when the current modulus is of maximum value. For the case investigated previously,  $p = 1$ , the sheet was found to be approximately of equal dimensions along  $x$  and  $y$ , the two coordinate directions associated with the fan surface. Looking at the figure, one can to see the difference between the current sheet at  $p = 0.1$  and at  $p = 10$  at the maximum current. We find the current sheet at  $p = 0.1$  large, being very extended along the  $x$ -axis, that is, the direction along which  $\mathbf{J}$  and the parallel electric field lie. However, this length decreases when  $p$  is increased, that is mean the current sheet is continue to grow in length when  $p$  decreases. The results suggest that when the value of  $p$  goes zero, the current sheet will grow indefinitely in the plane perpendicular to the shear, i.e. the direction of current flow through the null ( $x$ -direction). Note that with respect to the field strength in the fan plane, decreasing  $p$  corresponds to weaker magnetic field strength along the  $x$ -direction. Thus the extension of the current sheet could be attributed to the fact that the weak field region extends in that direction and the magnetic field becomes less able to resist the collapse to form the current layer. That is, when the magnetic field parallel to the current becomes weaker there is less magnetic pressure associated with this ‘guide field’ component in the current sheet away from the null, and the current sheet is able to extend further away from the null.

The current was before localised to form the sheet in the begin parallel to the fan plane ( $x$ -axis), but over time, due to the influence of forces, the angle

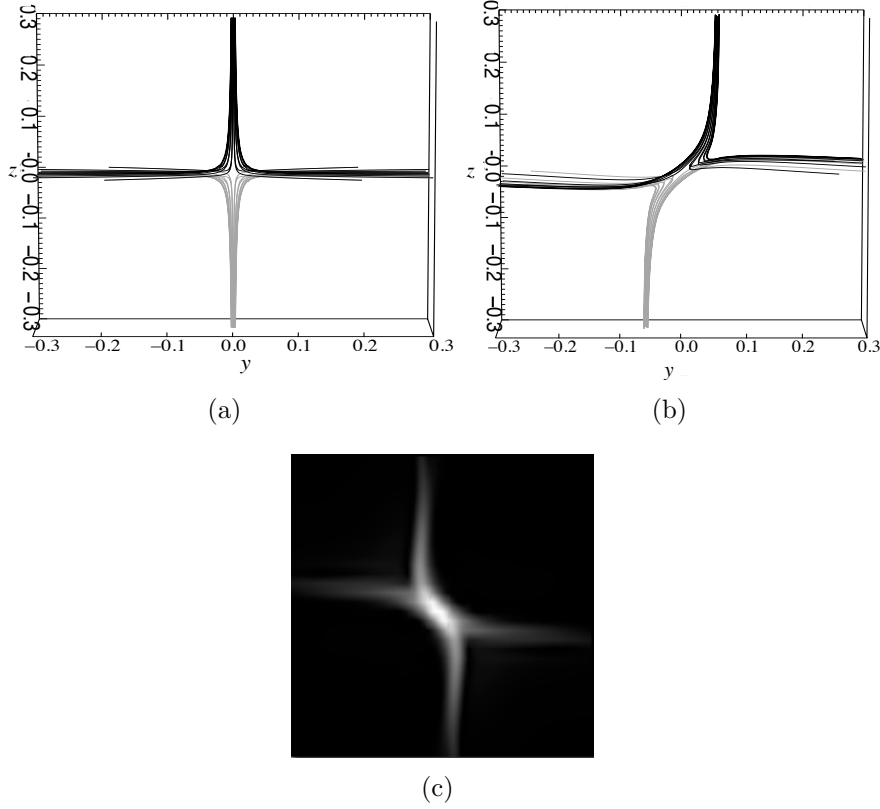


Figure 5: Structure of the magnetic field for the run with  $p = 2$  (a) at  $t = 0$ , and (b) at the time of maximum current ( $t = 3.0$ ), once the magnetic field has locally collapsed to form a current sheet. (c) Grayscale showing  $|\mathbf{J}|$  in the  $x = 0$  plane at the same time as (b).

between the fan plane and spine is beginning to change to become smaller and has led to the collapse of the null point to form the current sheet (see Fig. 5).

### 4.3 Maximum current attained

Figure 7(a) illustrates the evolution of the current modulus maximum within the domain in time, for runs with different values of the parameter  $p$ . We notice in each case the current  $|\mathbf{J}|$  growing sharply with time has reached to the maximum value, and then decreasing, as discussed above. In figure (7(b)) shows the evolution of maximum value of current  $|\mathbf{J}|$  near the null point with different values of  $p$ , we notice there is positive correlation be-

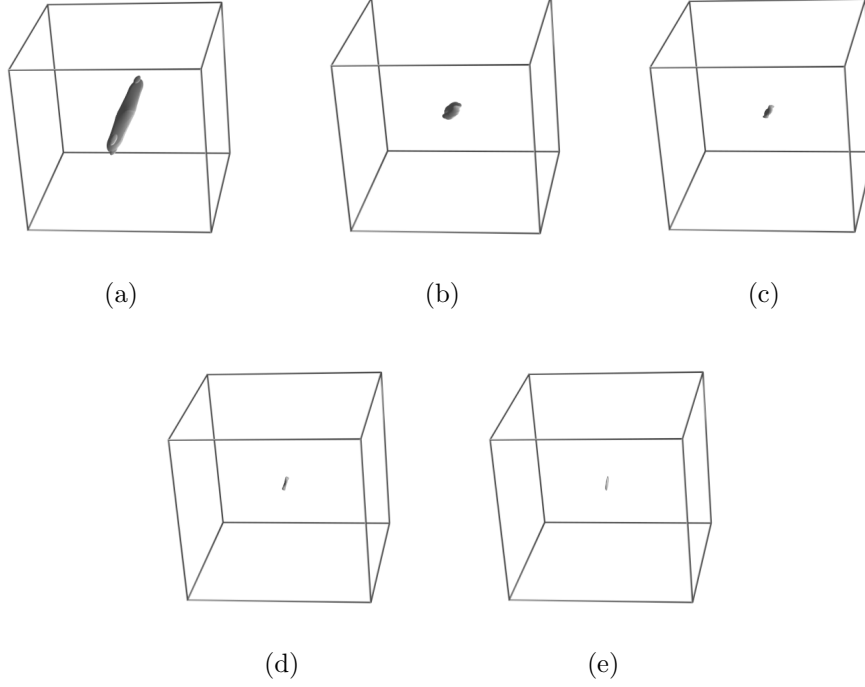


Figure 6: Isosurfaces of  $J$ , at 50% of the maximum at that time showing dimension of current sheet at different  $p$  and time, (a) current sheet in the time of maximum  $|J|$  at  $p = 0.1$ . (b) current sheet in the time of maximum  $|J|$  at  $p = 0.5$ . (c) current sheet in the time of maximum  $|J|$  at  $p = 1$ . (d) current sheet in the time of maximum  $|J|$  at  $p = 2$ . (e) current sheet in the time of maximum  $|J|$  at  $p = 10$ .

tween  $p$  and maximum current, on the other words, when the  $p$  increase then the maximum value of current also increase. Furthermore there is negative correlation between the size of current sheet and values of  $p$ , see figure (6). Thus, although the current becomes more localised as  $p$  increases, it also becomes more intense.

#### 4.4 Reconnection rate

In this section we calculate the reconnection rate, i.e. the amount of flux transported across the fan surface, as before by integrating the electric field component parallel to the magnetic field ( $E_{\parallel}$ ). Similarly to above, by symmetry, the integral is performed along the field line lying along the  $x$ -axis,

$$F = \int E_{\parallel} dy, \quad (35)$$

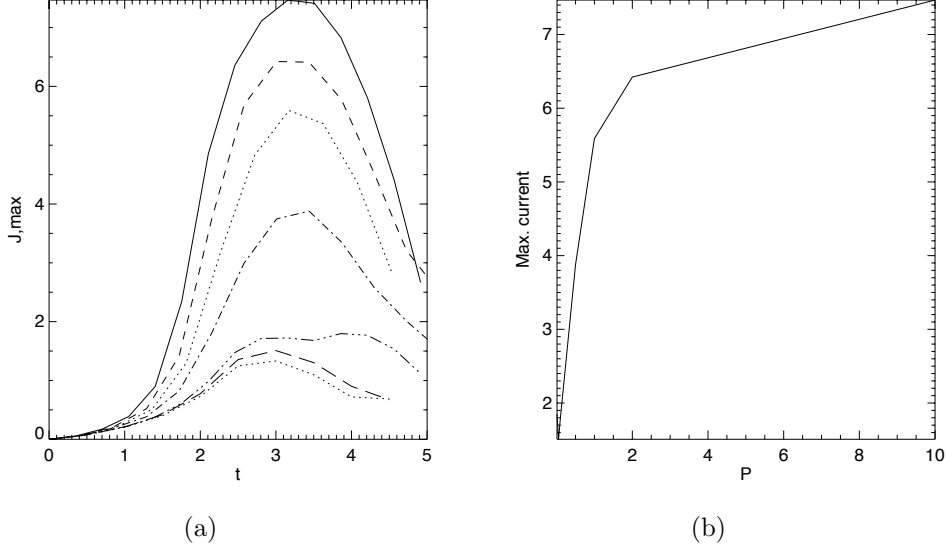


Figure 7: (a) Evolution of maximum value of  $|J|$  in time with different  $p$  where ( $J$  dotted at  $p = 0.01$ ,  $J$  long dashed at  $p = 0.05$ ,  $J$  dashed dot dot at  $p = 0.1$ ,  $J$  dashed dot at  $p = 0.5$ ,  $J$  dotted at  $p = 1$ ,  $J$  dashed at  $p = 2$ ,  $J$  solid at  $p = 10$ ). (b) to show the evolution of current with different  $p$ .

where since we are in the resistive MHD regime we have  $E_{\parallel} = \eta \mathbf{J} \cdot \mathbf{B} / |\mathbf{B}|$ .

In figure 8 we show the evolution of the reconnection rate in time with different values of  $p$ . Initially the rate clearly stay constant (zero) in time, in the other words during the early evolution, between  $t = 0$  and  $t = 1$ . Later, it starts to develop until it gains its maximum value, and then begins to decrease. This follows the same pattern as the evolution of the current, being indicative of the fact that the null point is collapse to form the current sheet, and then the system relaxing once the driving ceases. It is clear from Fig. 8 that the maximum reconnection rate attained increases as the value of  $p$  is decreased. It should be noted here that although our intuition tells us that there is positive correlation between current and reconnection rate, by contrast in this work we notice the inverse its true i.e. when the maximum current increases the reconnection rate is decreased. this is because the diffusion region is stretch when the  $p$  is tends to zero in the direction when the  $E_{\parallel}$  lies, therefore the rate is growth even though the current is decreasing, since the integrand in equation 35 is non-zero over a much larger portion of the  $x$ -axis.

If we finally compare our results with those of the incompressible model of Craig and Fabling (1998), we find their results differ from our results in terms



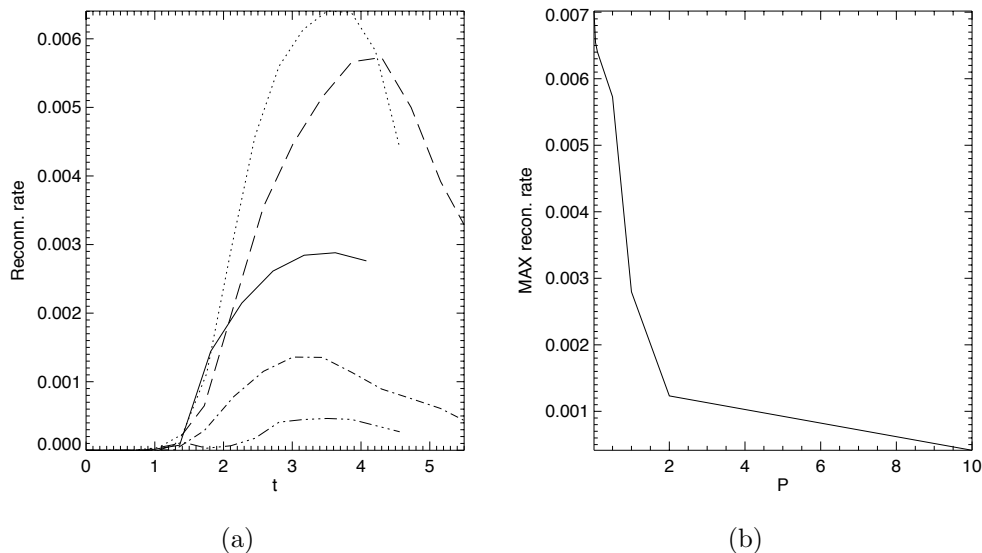


Figure 8: (a) Reconnection rate at different values of  $p$ , where dotted curve reconnection rate at  $p=0.1$ , long dashed curve at  $p=0.5$ , solid curve at  $p=1$ , dashed dot curve at  $p=2$  and dashed dot dot curve at  $p=10$ . (b) Variation of the maximum reconnection rate with the parameter  $p$ .

of the dependence of the peak current on  $p$ . In particular, they found that (in terms of our parameters) the maximum current decreases when  $p$  goes to infinity. This may be down to the very different geometries of the current sheet in the two models (the current sheet in the incompressible model is planar and extends to infinity along the fan for all values of  $p$ ). However, it is of interest to note that we actually find the same behavior of reconnection rate with  $p$ , i.e. as  $p$  decreases the reconnection rate increases (since in fact we find a negative correlation between  $J_{max}$  and the reconnection rate as  $p$  is varied).

## 5 Conclusions and Discussion

In this paper we have investigated the effect of the symmetry of the magnetic field on magnetic reconnection at an isolated null point. We concentrate on the so-called spine-fan mode of null point reconnection at 3D null points: effect of magnetic field asymmetry. In the first part of the paper we discussed a steady solution of the kinematic resistive MHD equations, which exist around the magnetic null point with generalised magnetic field

$\mathbf{B}=B'_0(x, py - jz, -(p+1)z)$ . This magnetic field has current aligned to the fan surface of the null point, and Pontin et al. (2005) investigated this situation in the non-generic symmetric case  $p = 1$ . In this work we use  $p$  as a parameter. We found the plasma flow, and the resulting qualitative structure of the reconnection process to be the same as found in the symmetric case (Pontin et al., 2005). Specifically, we found plasma flow across both the spine line and fan plane of the null for all values of  $p$ .

We then described the results of a computational resistive MHD simulation in which we investigated the nature of MHD evolution with the different values of  $p$ , and current sheet formation at 3D generalised magnetic nulls. In addition to the current sheet at the null, a condition that reconnection should take place there is given by the presence of localised parallel electric field. The maxima of this parallel electric field occur along the  $x$ -axis. The integral of  $E_{\parallel}$  along the field line which is coincident with this axis (by symmetry) gives the reconnection rate (Pontin et al., 2005).

We went to investigate the process of current sheet formation at such three dimension null in the two solution. We found in our simulation strong current focused at the null. By necessity, as the dynamics of the system are not included in our steady-state kinematic solution, a current is imposed, which has the same orientation at the null as found in the simulations (the orientation of  $\mathbf{J}$  at the null has been shown to be the crucial quantity in determining the topological structure of the reconnection process (Pontin et al., 2004, 2005). In order that the diffusion region is localised in both cases, a localised resistivity was imposed in the kinematic solution.

One of the major results that arises from the sequence of simulations is that both the peak intensity and the dimensions of current sheet are strongly dependent on the symmetry/asymmetry of the field, or in other words on the value of  $p$ . In terms of the dimensions, the length along the direction of current flow at the null increases when  $p$  goes to zero, i.e. the diffusion region is stretched in the direction of  $z$  when  $p$  tends to zero. In the kinematic solution it was also possible by choosing the correct parameters to have the diffusion region have such a  $p$ -dependence.

In addition to the current sheet at the null, we examined the reconnection rate, in both solutions. In kinematic solution, the dependence of the reconnection rate on  $p$  is strongly dependent on the parameters chosen. We found that as  $p \rightarrow \infty$  the reconnection rate approaches some constant value when  $|\mathbf{J}|$  is held fixed. In contrast as  $p \rightarrow 0$ , the reconnection rate either approaches zero ( $a \leq 1$ ) or tends to infinity ( $a > 1$ ). The results of the simulation suggest that the parameter range  $a > 1$  is the most realistic since it was found that the diffusion region is stretched along the direction of current flow ( $x$ ) when  $p$  decreases – see figure (6) – which leads to the reconnection

rate approaching infinity.

## 6 Acknowledgments

We would like to thank G. Hornig, A. L. Wilmot-Smith and E. R. Priest for helpful and stimulating discussions. A.K.H. Al-Hachami was supported in this work by a grant from the Iraqi Government. Computational simulations were developed in conjunction with K. Galsgaard, and run on the MHD Computing Consortium's Beowulf cluster.

## References

- Barnes, G. (2007). On the relationship between coronal magnetic null points and solar eruptive events. *Astrophys. J. Lett.*, 670:L53–L56.
- Craig, I. J. D. and Fabling, R. B. (1998). Dynamic magnetic reconnection in three space dimensions: Fan current solutions. *Phys. Plasmas*, 5:635–644.
- Demoulin, P. (2006). Extending the concept of separatrices to qsfs for magnetic reconnection. *Cospar*, 37:1269–1282.
- Fletcher, L., Metcalf, T. R., Alexander, D., Brown, D. S., and Ryder, L. A. (2001). Evidence for the flare trigger site and three-dimensional reconnection in multiwavelength observations of a solar flare. *Astrophys. J.*, 554:451–463.
- Fukao, S., Ugai, M., and Tsuda, T. (1975). Topological study of magnetic field near a neutral point. *Rep. Ion. Sp. Res. Japan*, 29:133–139.
- Galsgaard, K. and Nordlund, A. (1997). Heating and activity of the solar corona: 3. dynamics of a low beta plasma with 3d null points. *J. Geophys. Res.*, 102:231–248.
- Hesse, M. (1991). In advances in solar system magnetohydrodynamics. *Cambridge University Press: Cambridge*, page 221.
- Hornig, G. and Priest, E. R. (2003). Evolution of magnetic flux in an isolated reconnection process. *Physics of Plasmas*, 10:2712–2721.
- Klapper, I., Rado, A., and Tabor, M. (1996). A lagrangian study of dynamics and singularity formation at magnetic null points in ideal three-dimensional magnetohydrodynamics. *Phys. Plasmas*, 3(11):4281–4283.

- Lau, Y. T. and Finn, J. M. (1990). Three dimensional kinematic reconnection in the presence of field nulls and closed field lines. *Astrophys. J.*, 350:672–691.
- Longcope, D. W. (1996). Topology and current ribbons: a model for current, reconnection and flaring in a complex evolving corona,. *Solar Phys.*, **169**:91–121.
- Longcope, D. W. (2001). Separator current sheets: Generic features in minimum-energy magnetic fields subject to flux constraints. *Physics of Plasmas*, **8**:5277–5290.
- Longcope, D. W., Brown, D. S., and Priest, E. R. (2003). On the distribution of magnetic null points above the solar photosphere. *Phys. Plasmas*, 10:3321–3334.
- Longcope, D. W. and Cowley, S. C. (1996). Current sheet formation along three-dimensional magnetic separators. *Phys. Plasmas*, 3:2885–2897.
- Luoni, M. L., Mandrini, H. H., Cristiani, G. D., and Démoulin, P. (2007). The magnetic eld topology associated with two m ares. *Adv. Space Res.*, 39:1382–1388.
- Parnell, C. E., Smith, J. M., Neukirch, T., and Priest, E. R. (1996). The structure of three-dimensional magnetic neutral points. *Phys. plasmas*, **3**(3):759–770.
- Pontin, D. I., Bhattacharjee, A., and Galsgaard, K. (2007). Current sheet formation and non-ideal behaviour at three-dimensional magnetic null points. *Phys. Plasmas*, 14:052106.
- Pontin, D. I. and Craig, I. J. D. (2005). Current singularities at finitely compressible three-dimensional magnetic null points. *Phys. Plasmas*, 12:072112.
- Pontin, D. I. and Galsgaard, K. (2007). Current amplification and magnetic reconnection at a 3d null point. physical characteristics. *J. Geophys. Res.*, 112:A03103.
- Pontin, D. I., Hornig, G., and Priest, E. R. (2004). Kinematic reconnection at a magnetic null point: Spine-aligned current. *Geophys. Astrophys. Fluid Dynamics*, 98:407–428.

- Pontin, D. I., Hornig, G., and Priest, E. R. (2005). Kinematic reconnection at a magnetic null point: Fan-aligned current. *Geophys. Astrophys. Fluid Dynamics*, 99:77–93.
- Priest, E. R. and Forbes, T. G. (2000). *Magnetic reconnection: MHD theory and applications*. Cambridge University Press, Cambridge.
- Priest, E. R., Hornig, G., and Pontin, D. I. (2003). On the nature of three-dimensional magnetic reconnection. *J. Geophys. Res.*, 108(A7):SSH6–1.
- Priest, E. R., Longcope, D. W., and Heyvaerts, J. F. (2005). Coronal heating at separators and separatrices. *Astrophys. J.*, 624:1057–1071.
- Priest, E. R. and Pontin, D. I. (2009). 3d null point reconnection regimes. submitted to *Phys. Plasmas*.
- Priest, E. R. and Titov, V. S. (1996). Magnetic reconnection at three-dimensional null points. *Phil. Trans. R. Soc. Lond. A*, 354:2951–2992.
- Rickard, G. J. and Titov, V. S. (1996). Current accumulation at a three-dimensional magnetic null. *Astrophys. J.*, 472:840–852.
- Schindler, K., Hesse, M., and Birn, J. (1988). General magnetic reconnection, parallel electric fields, and helicity. *J. Geophys. Res.*, 93(A6):5547–5557.
- Schrijver, C. J. and Title, A. M. (2002). The topology of a mixed-polarity potential field, and inferences for the heating of the quiet solar corona. *Solar Phys.*, 207:223–240.
- Ugarte-Urra, I., Warren, H. P., and Winebarger, A. R. (2007). The magnetic topology of coronal mass ejection sources. *Astrophys. J.*, 662:1293–1301.
- Wilmot-Smith, A.L., Hornig, G., and Priest, E. (2009). Dynamic non-null magnetic reconnection in three-dimensions - ii. composite solutions. *Geophys. Astrophys. Fluid Dyn.*, in press.
- Wilmot-Smith, A. L., G.Hornig, and Priest, E. R. (2006). Dynamic non-null magnetic reconnection in three dimensions. i. particular solutions. *Proc. R. Soc. A*, **462**:2877–2895.
- Xiao, C. J., Wang, X. G., Pu, Z. Y., Zhao, H., Wang, J. X., Ma, Z. W., Fu, S. Y., Kivelson, M. G., Liu, Z. X., Zong, Q. G., Glassmeier, G. H., Balogh, A., Korth, A., Reme, H., and Escoubet, C. P. (2006). In situ evidence for the structure of the magnetic null in a 3d reconnection event in the earth’s magnetotail. *Nature Physics*, 2:478–483.